# Magnetic Pressure Support and Accretion Disk Spectra

Omer M. Blaes and Shane W. Davis

Department of Physics, University of California, Santa Barbara, CA 93106

blaes@physics.ucsb.edu, swd@physics.ucsb.edu

Shigenobu Hirose

Earth Simulator Center, JAMSTEC, 3173-25 Showa-machi, Kanazawa-ku, Yokohama, Kanagawa 236-0001, Japan

shirose@jamstec.go.jp

Julian H. Krolik

Department of Physics and Astronomy, Johns Hopkins University, Baltimore, MD 21218

jhk@pha.jhu.edu

and

James M. Stone

Department of Astrophysical Sciences, Princeton University, Princeton, NJ 08544

jstone@astro.princeton.edu

## ABSTRACT

Stellar atmosphere models of ionized accretion disks have generally neglected the contribution of magnetic fields to the vertical hydrostatic support, although magnetic fields are widely believed to play a critical role in the transport of angular momentum. Simulations of magnetorotational turbulence in a vertically stratified shearing box geometry show that magnetic pressure support can be dominant in the upper layers of the disk. We present calculations of accretion disk spectra that include this magnetic pressure support, as well as a vertical dissipation profile based on simulation. Magnetic pressure support generically produces a more vertically extended disk atmosphere with a larger density scale height. This acts to harden the spectrum compared to models that neglect magnetic pressure support. We estimate the significance of this effect on disk-integrated spectra by calculating an illustrative disk model for a stellar mass black hole, assuming that similar magnetic pressure support exists at all radii. Subject headings: accretion, accretion disks — MHD — radiative transfer — X-rays: binaries

## 1. Introduction

Almost without exception, models of geometrically thin accretion disks that are used to predict radiation spectra in order to compare with observation are based on the alpha prescription introduced by Shakura & Sunyaev (1973). This prescription enables one to compute the radial distribution of surface density in the disk. When this is combined with additional assumptions about the vertical distribution of dissipation, complete models of the vertical structure at each radius and the local radiation spectrum can be computed.

In black hole accretion disks, for example, the most detailed of such models so far are those of Hubeny et al. (2001) for supermassive black holes, Davis et al. (2005) for stellar mass black holes, and Hui, Krolik, & Hubeny (2005) for intermediate mass black holes. The models fully account for relativistic effects, and include a detailed non-LTE treatment of level populations of hydrogen, helium, and abundant metals. Continuum opacities due to bound-free and free-free transitions, as well as Comptonization, are included. In spite of this level of sophistication, the models are limited by other assumptions: the disk is assumed to be stationary, the alpha-prescription is used to calulate the radial distribution of surface density, a no-torque inner boundary condition is assumed, the vertical structure at each radius is assumed to depend only on height and is symmetric about the midplane, the vertical distribution of dissipation per unit mass is assumed to be constant, and the disk is assumed to be supported vertically against the tidal field of the black hole by just gas and radiation pressure.

It is now widely believed that the anomalous stress in accretion disks is a result of sustained magnetohydrodynamical turbulence which is akin to that seen in the nonlinear development of the magnetorotational instability, or MRI (Balbus & Hawley 1998). In principle, shearing box simulations of this turbulence which incorporate the vertical tidal field of the central mass (Brandenburg et al. 1995; Stone et al. 1996; Miller & Stone 2000) can be used to build models of the vertical structure of accretion disks that are free of the ad hoc assumptions that plague existing models. The most recent of these simulations (Turner 2004; Hirose, Krolik, & Stone 2005) are particularly useful for this purpose as they evolve the equations of radiation magnetohydrodynamics and have self-consistent thermodynamics. While much of the dissipation of the turbulence in these simulations is numerical and happens on the grid scale, one hopes that this still mocks up the microscopic dissipation occuring at the smallest scales of the turbulent cascade, and in any case provides a better handle on the true spatial distribution of dissipation than the ad hoc assumptions used in alphadisk models. Moreover, in radiation pressure dominated simulations of MRI turbulence, dissipation of compressive motions by photon diffusion is fully resolved (Turner et al. 2003).

Davis et al. (2005) used the time and horizontally-averaged vertical dissipation profile from the simulation of Turner (2004) to compute the vertical structure and spectrum of an annulus, and compared it to a model based on the usual ad hoc assumption of constant dissipation per unit mass. While the resulting profiles of density and temperature were very different, the emergent spectrum was very similar. In fact, Davis et al. (2005) found that the locally emergent spectra of individual annuli were remarkably robust to different vertical dissipation profiles and to different overall stress prescriptions, provided most of the dissipation occurs deeper than the effective photosphere. Part of this robustness stems from the fact that the radiative flux becomes constant above the dissipation region, and so the radiative force per unit mass also becomes constant if the flux mean opacity is dominated by electron scattering in the surface layers. Because the tidal gravity of the central mass increases with height, gas pressure gradients must therefore compensate, and this results in very steep density gradients near the photosphere. The density and temperature at the effective photosphere then become roughly independent of the details of the vertical structure, resulting in a robust emergent spectrum.

In addition to a markedly different dissipation profile, vertically stratified MRI simulations also show that the surface layers of a disk will be *magnetically* supported. This additional support removes the need for steep density gradients, and in fact results in a much more extended atmosphere with a larger density scale height. As qualitatively suggested by Hirose, Krolik, & Stone (2005), magnetic pressure support could therefore dramatically alter the emergent spectrum, much more than alterations of the dissipation profile deeper than the effective photosphere. It is this new effect arising from MRI simulations that we investigate in this paper.

In section 2, we discuss the time and horizontally-averaged dissipation and magnetic pressure profiles that we computed from the simulations. We then used these profiles within the stellar atmosphere code TLUSTY (Hubeny 1988; Hubeny & Lanz 1995) to compute the vertical structure and emergent spectrum of individual annuli. We present the results of these calculations in section 3, including an illustrative whole disk spectrum for an accreting stellar mass black hole. We then summarize our conclusions in section 4.

#### 2. Vertical profiles of magnetic pressure and dissipation

Hirose, Krolik, & Stone (2005) started with an initial condition corresponding to an annulus at 300  $GM/c^2$  around a black hole of mass  $M = 6.62 \,\mathrm{M_{\odot}}$ . The surface density of the annulus matched that of a Shakura-Sunyaev disk with  $\alpha = 0.02$  and a luminosity equal to 0.066 times the Eddington rate, assuming 10 percent radiative efficiency. After including a weak magnetic field with no net poloidal flux, the MRI grows and produces turbulence which saturates by about ten orbits, and a rough balance between heating and radiative cooling is thereafter established until a numerical problem at the boundaries interferes at about 60 orbits. At any specific time, thermal balance is not exact, as there are significant fluctuations in both heating and radiative cooling. In addition, significant asymmetries above and below the midplane exist, and the flux emerging from one side can exceed that from the other by factors of 2-3 over time scales as long as 5-10 orbits. Spatial variations in the horizontal direction come and go as well.

It would be interesting in future to compute the instantaneous emergent spectrum from the annulus using three dimensional, time and frequency-dependent radiative transfer, but our scope here is much less ambitious. We simply wish to examine the overall effects of the dissipation and magnetic pressure profiles on the time-averaged spectrum. We therefore horizontally averaged all fluid quantities in the simulation at every time step, and then computed a time average from 10 to 60 orbits of these variables at every height. We tried two types of averages of quantities related to energy and pressure (e.g flux, pressure gradients, dissipation rate): a straight time average and a time average weighted by the total instantaneous magnetic plus thermal energy in the annulus. Both approaches gave very nearly identical results.] The time-averaged profiles still had small asymmetries about the midplane (as much as 20 percent in the case of the magnetic pressure gradients), so as a final step, we averaged all the vertical profiles above and below the disk midplane. The surface density and emergent flux from the resulting averaged structure still matches that of a Shakura-Sunyaev annulus at a radius of  $300GM/c^2$  around a 6.62 M<sub> $\odot$ </sub> black hole, now accreting at  $1.1 \times 10^{18}$  g/s (corresponding to a luminosity of 0.095 in units of Eddington for 10 percent radiative efficiency) and with  $\alpha = 0.016$ .

Figure 1 depicts the average energy dissipation per unit mass  $\epsilon$ , together with the average vertical radiative flux gradient divided by density:  $\rho^{-1}dF/dz = -dF/dm$ , as a function of column mass density m measured from the surface inward. In a stationary, one-dimensional structure, radiative equilibrium would require these two profiles to be identical, but the average profiles from the simulation are not quite in such agreement.

Following Hubeny & Hubeny (1998), we fit the profile of dF/dm with a broken power

law,

$$\frac{dF}{dm} = -\left(\frac{F(0)}{m_0}\right) \frac{(\zeta_0 + 1)(\zeta_1 + 1)}{(\zeta_0 - \zeta_1)(m_d/m_0)^{\zeta_0 + 1} + \zeta_1 + 1} \begin{cases} (m/m_0)^{\zeta_1}(m_d/m_0)^{\zeta_0 - \zeta_1}, & \text{if } m < m_d; \\ (m/m_0)^{\zeta_0}, & \text{if } m > m_d. \end{cases}$$
(1)

Here  $F(0) = 4.37 \times 10^{18}$  erg cm<sup>-2</sup> s<sup>-1</sup> is the average flux emerging from one face of the annulus and  $m_0 = 4.88 \times 10^4$  g cm<sup>-2</sup> is the midplane column density of the annulus (i.e. half the total surface mass density). The dimensionless parameters for this fit were  $\zeta_0 = -0.6$ ,  $\zeta_1 = 0$ , and  $(m_d/m_0) = 4 \times 10^{-5}$ , and we compare the fit to the simulation data in Figure 1. Both the derivative dF/dm from equation (1) and its analytic integral F(m) are used in constructing the atmosphere model, because the radiative equilibrium equation in the code TLUSTY is used in both integral and differential form (Hubeny & Lanz 1995).

Note that  $|mdF/dm| \propto m^{0.4}$  at high column densities, so that most of the integrated dissipation in the annulus occurs at high column density and low altitude, as Hirose, Krolik, & Stone (2005) point out. While Figure 1 demonstrates that the highest values of dissipation per unit mass actually occur at high altitudes and low column densities, this does not significantly affect the emergent spectrum. Figure 2 compares the emergent spectrum assuming a constant dissipation per unit mass with the dissipation profile of equation (1). The results are virtually identical, although the spectrum based on equation (1) actually differs in having a faint, hard tail at high energies. This is not shown in Figure 2 as it starts too far into the tail of the spectrum. The hard tail results from the fact that the new dissipation profile produces a high temperature region at very low column densities, as shown in Figure 6 below. In any case, provided most of the dissipation occurs deeper than the effective photosphere, the resulting spectrum near the spectral peak does not appear to depend sensitively on how the dissipation is distributed. This is perhaps not surprising, and Davis et al. (2005) found very similar results when using the dissipation profile computed by Turner (2004), although the emergent spectra were not quite as close as here.

Figure 3 depicts the average vertical accelerations produced by magnetic pressure gradients  $dp_{\rm mag}/dm \equiv d/dm(B^2/8\pi)$ , gas pressure gradients dp/dm, and radiation pressure  $\chi F/c$ . Ignoring magnetic tension forces, the sum of these three should equal the magnitude of the local vertical gravitational acceleration if the structure was completely stationary and onedimensional. For column masses  $m > 10^2$  g cm<sup>-2</sup>, this is reasonably accurate, but there are strong deviations from this at lower column densities. Again, it is beyond the scope of this paper to compute the time-dependent spectrum from the simulations. In order to account for the effects of large magnetic pressure gradients in the upper layers, we determine the fractional contribution of each acceleration to the total at every location, and then rescale that fraction by the local gravity. The result is depicted in Figure 4. We then incorporate this profile of  $dp_{\rm mag}/dm$  in TLUSTY by mapping it directly onto the column density grid used in the code. In order to avoid the upper vertical boundary effects on the simulation data at low column densities (see the kinks in Figure 4 at  $m = 0.1 \text{ g cm}^{-2}$ ), we extrapolate  $dp_{\text{mag}}/dm$  as a constant for  $m < 0.1 \text{ g cm}^{-2}$ .

## 3. Spectra from magnetically supported disks

Figure 5 compares the emergent spectrum from the annulus when magnetic pressure support is or is not included in the vertical hydrostatic balance. In contrast to changing the dissipation profile (Figure 2), magnetic pressure support produces a much more noticeable change, and causes the spectrum to be significantly harder.

The reason for this can be seen in Figure 6, which shows the vertical density and temperature profiles in the two structures, as well as the locations of the effective photospheres at frequencies corresponding to the two spectral peaks. Without magnetic pressure support, large gas pressure gradients are required to support the disk against the high gravity at high altitude. These necessarily require steep density gradients because the temperature profile (largely set by radiative equilibrium) is too flat. Magnetic pressure support relaxes this constraint, permitting a much more extended density profile. Because the location of the effective photosphere is set by an approximately fixed column density, the larger density scale height in a magnetically supported annulus implies that the density at the effective photosphere will be lower than would be the case if magnetic pressure was neglected. The lower density reduces the ratio of absorption to scattering opacity, which alone would tend to harden the spectrum by producing a modified blackbody. In addition, the lower density implies that metals are more ionized than they would otherwise be, and this reduces the strength of absorption edges. This is illustrated in detail in Figure 7, which shows the non-LTE departure coefficient for the CVI ground state, which is responsible for the absorption edge feature at 0.5 keV in the unmagnetized spectrum. In the magnetized atmosphere, non-LTE effects reduce the ground state population of this ion even further, and drive the edge into emission. For all these reasons, we expect atmosphere calculations which include magnetic pressure support will generically result in harder spectra. This applies to electrically conducting accretion disks with MRI turbulence in all astrophysical contexts, from cataclysmic variables to active galactic nuclei.

Figure 6 also compares the time and horizontally averaged density and temperature structures from the Hirose, Krolik, & Stone (2005) simulation with those computed by TLUSTY. The density profiles are in excellent agreement, and even the temperatures compare favorably beneath the effective photosphere.

Observations of course do not measure the spectrum emitted locally at some radius in the disk, but the spectrum of the entire disk as carried by photons that reach detectors at infinity. To illustate how important magnetic pressure support might be on an observed system, we calculated the spectrum of a relativistic accretion disk around a black hole. This is a cleaner system than, e.g., a cataclysmic variable where boundary layer effects need to be included. However, we warn the reader that significant uncertainties still remain in our understanding of the nominally radiation pressure supported inner regions of luminous black hole accretion disks, uncertainties which we do not address here.

We chose a ten solar mass Schwarzschild hole, accreting at  $3.88 \times 10^{-8} M_{\odot}/\text{yr}$  (giving an Eddington ratio of  $L/L_{\text{Edd}} = 0.08$ ). We assume a standard Shakura-Sunyaev prescription, where the vertically integrated stress equals the vertically integrated total pressure (neglecting magnetic fields), times  $\alpha = 0.01$ .

We first calculated the vertical structure of each annulus neglecting magnetic pressure support but using the dissipation profile of equation (1). This determines a midplane pressure  $P_0$ . Then combining this with the surface mass density at the midplane  $m_0$  (determined from the vertically-integrated radial disk structure model), we rescaled our numerical magnetic pressure acceleration profile by  $P_0/m_0$ . We then used this rescaled magnetic pressure profile to calculate a new model for the annulus vertical structure. The resulting disk-integrated spectrum as seen by an observer at infinity at an inclination angle of 60° to the symmetry axis of the hole is shown in Figure 8. As expected, adding magnetic pressure support hardens the spectrum.

In order to quantify the degree of hardening, we fit the spectrum above 0.1 keV to relativistic, multitemperature blackbody disk models with a constant color correction factor f, defined such that the local specific intensity is given by an isotropic, color corrected blackbody:  $I_{\nu} = B_{\nu}(fT_{\rm eff})/f^4$ , where  $B_{\nu}$  is the Planck function and  $T_{\rm eff}$  is the local effective temperature. We fixed the mass, Eddington ratio, and disk inclination in these fits, only allowing f and the overall normalization to vary. (Allowing the normalization to vary is necessary as the actual model spectrum is limb-darkened.) The fitted color correction factor was 1.74 for the magnetized spectrum, and 1.48 for no magnetic fields. We also tried fitting the spectra above 0.1 keV to relativistic disk atmosphere models around stellar mass black holes with  $\alpha = 0.01$  (Davis et al. 2005; Davis & Hubeny 2005). In these fits we again fixed the mass, Eddington ratio, and disk inclination. We also fixed the overall normalization, as the relativistic disk atmosphere models account for limb-darkening. Only the black hole spin was allowed to vary. The best fit spin for the unmagnetized model was a/M = 0.05, which is consistent with the fact that the modified dissipation profile in equation (1) does not produce much change in the overall spectrum. For the magnetized disk model, however,

we found the best fit spin to be a/M = 0.46, due to its harder spectrum. Because limb darkening has some spin-dependence, we also redid the fits with free normalization, but still got very similar best-fit spins.

#### 4. Discussion and conclusions

The advent of thermodynamically self-consistent simulations of MRI turbulence in vertically stratified shearing boxes (Turner 2004; Hirose, Krolik, & Stone 2005) has finally opened the door to the construction of spectral models which are based on the physics of the turbulence itself. Surprisingly, our investigation in this paper indicates that the thermodynamics itself, i.e. the vertical profile of dissipation, has little effect on the emergent spectrum compared to models based on the standard assumption of a constant dissipation rate per unit mass. This conclusion was also reached in the earlier investigation of Davis et al. (2005). Unless an annulus in the disk is only moderately effectively thick, most of the dissipation occurs deeper than the effective photosphere, and its vertical profile therefore has little effect on the emergent spectrum. The reader should bear in mind, however, that the numerical dissipation profiles, e.g. equation (1), are based on simulations in which mechanical energy is simply lost at the grid scale and replaced by internal energy. More work needs to be done to investigate whether these profiles are robust to changes in grid resolution. In addition, the simulations were for gas pressure dominated annuli, and large uncertainties still remain to be fully investigated in the radiation pressure dominated case, which is more relevant for the innermost annuli of luminous accretion disks around black holes and neutron stars.

In contrast to the thermodynamics, the actual *dynamics*, i.e. the contribution of magnetic pressure to the vertical support of the disk against gravity, does produce significant changes in the emergent spectrum when compared to models based on the standard ad hoc assumptions. Magnetic pressure support at high altitude results in a much more extended density scale height, because gas pressure is not required to support the atmosphere against the increasing vertical gravity at high altitude. Because absorption opacity generally increases with density, a larger density scale height results in a smaller density at the effective photosphere in order to produce the same effective optical depth of unity. As anticipated by Hirose, Krolik, & Stone (2005), this enhances non-LTE effects in the spectrum because collisional processes in the plasma are then diminished compared to radiative processes. Even in LTE, lower density at the effective photosphere generally implies that the plasma becomes more ionized, reducing the bound-free opacity. Electron scattering is enhanced compared to absorption, driving the emergent radiation spectrum closer to a modified blackbody. All of these effects mean that the emergent spectrum will be generically harder compared to an atmosphere where magnetic support is neglected.

We emphasize that these spectral implications will apply to all accretion disks in which the MRI is thought to act, including active galactic nuclei, cataclysmic variables, and Xray binaries. In the one whole disk model we constructed, around a stellar mass black hole, we found that the magnitude of this hardening was equivalent to choosing a color correction factor in a relativistic, multitemperature blackbody of 1.74, as opposed to 1.48 in the nonmagnetized case. This has important implications for recent attempts to measure black hole spins in X-ray binaries by continuum spectral fitting (e.g. Shafee et al. 2005). Because magnetic pressure support hardens the spectrum, the fitted black hole spin to the observed continuum will have to compensate by being smaller.

It is conceivable that magnetic pressure support may be exaggerated in the local shearing box simulations. Long wavelength Parker instability modes might be suppressed because they cannot fit inside the box. This is an issue which will need further investigation, but we did a preliminary check by comparing with global, non-radiative, general relativistic MRI simulations (De Villiers, Hawley, & Krolik 2003). In the shearing box simulations, magnetic pressure becomes dominant when the density falls below 0.03 times the midplane density. In contrast, in a global simulation in Schwarzschild geometry, the magnetic pressure becomes dominant below 0.1 times the local midplane density. Magnetic support therefore appears to be even more important in the global simulation which, however, was non-radiative.

The shearing box simulations show significant time-dependence, horizontal structure, and asymmetries above and below the disk midplane, effects which we have ignored by ruthless averaging. More sophisticated radiative transfer techniques will have to be employed to investigate their effect on the emergent spectrum. Density irregularities in particular are expected to be even more prominent in the radiation pressure dominated inner regions of black hole accretion disks (Turner et al. 2003; Turner 2004; Turner et al. 2005). Monte Carlo simulations of the photon transfer through such inhomogeneous structures suggest that the enhanced ratio of absorption to scattering opacity in the denser regions helps to thermalize (and therefore soften) the emergent spectrum (Davis et al. 2004), at least when the inhomogeneities are treated as static structures. Whether or not this persists in a timedependent calculation, or whether or not the hardening due to magnetic pressure support turns out to be the more important effect, remains to be seen.

This research was supported by the National Science Foundation under grant nos. PHY99-07949 and AST 03-07657, and by NASA under grant no. NAG5-13228.

#### REFERENCES

- Balbus, S. A., & Hawley, J. F., 1998, Rev. Mod. Phys., 70, 1
- Brandenburg, A., Nordlund, Å, Stein, R. F., & Torkelsson, U., 1995, ApJ, 446, 741
- Davis, S., Blaes, O., Turner, N., & Socrates, A., 2004, in AGN Physics with the Sloan Digital Sky Survey, ASP Conference Series, G. T. Richards & P. B. Hall, eds., 135
- Davis, S. W., Blaes, O. M., Hubeny, I., & Turner, N. J., 2005, ApJ, 621, 372
- Davis, S. W., & Hubeny, I., 2005, ApJ, submitted
- De Villiers, J.-P., Hawley, J. F., & Krolik, J. H., 2003, ApJ, 599, 1238
- Hirose, S., Krolik, J. H., & Stone, J. M., 2005, ApJ, submitted
- Hui, Y., Krolik, J. H., & Hubeny, I., 2005, ApJ, 625, 913
- Hubeny, I., 1988, Comp. Phys. Commun., 52, 103
- Hubeny, I., & Lanz, T., 1995, ApJ, 439, 875
- Hubeny, I., & Hubeny, V., 1998, ApJ, 505, 558
- Hubeny, I., Blaes, O., Krolik, J. H., & Agol, E., 2001, ApJ, 559, 680
- Miller, K. A., & Stone, J. M., 2000, ApJ, 534, 398
- Shafee, R., McClintock, J. E., Narayan, R., Davis, S. W., Li, L.-X., & Remillard, R. A., 2005, ApJ, in press
- Shakura, N. I., & Sunyaev, R. A., 1973, A&A, 24, 337
- Stone, J. M., Hawley, J. F., Gammie, C. F., & Balbus, S. A., 1996, ApJ, 463, 656
- Turner, N. J., 2004, ApJ, 605, L45
- Turner, N. J., Stone, J. M., Krolik, J. H., & Sano, T., 2003, ApJ, 593, 992
- Turner, N. J., Blaes, O. M., Socrates, A., Begelman, M. C., & Davis, S. W., 2005, ApJ, 624, 267

This preprint was prepared with the AAS LATEX macros v5.2.

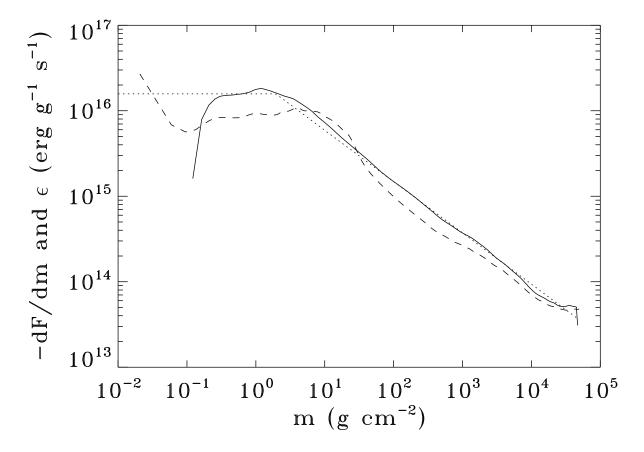


Fig. 1.— Time and horizontally-averaged profiles of the vertical flux gradient  $\rho^{-1}dF/dz = -dF/dm$  (solid) and energy dissipation rate per unit mass  $\epsilon$  (dashed) as functions of column mass density m, from the Hirose, Krolik, & Stone (2005) simulation. The dotted curve is the broken power law fit from equation (1) that we use in our spectral computation.

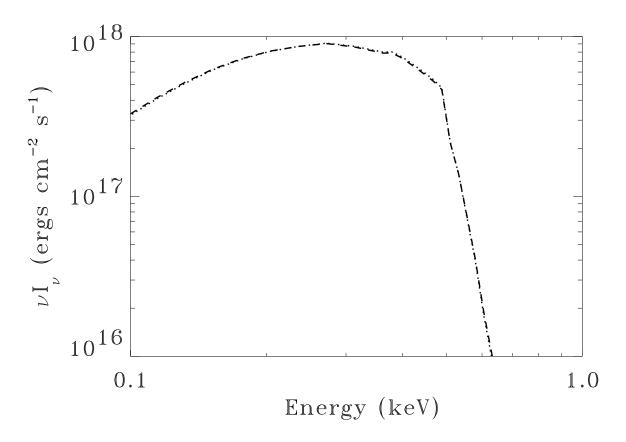


Fig. 2.— Local emergent spectrum in the fluid rest frame from the disk annulus viewed at an inclination angle of  $55^{\circ}$  from the disk normal. The dotted curve is based on the standard assumption of constant dissipation per unit mass, while the dashed curve uses the vertical dissipation profile of equation (1) based on simulation. Magnetic pressure support is neglected in both cases shown here.

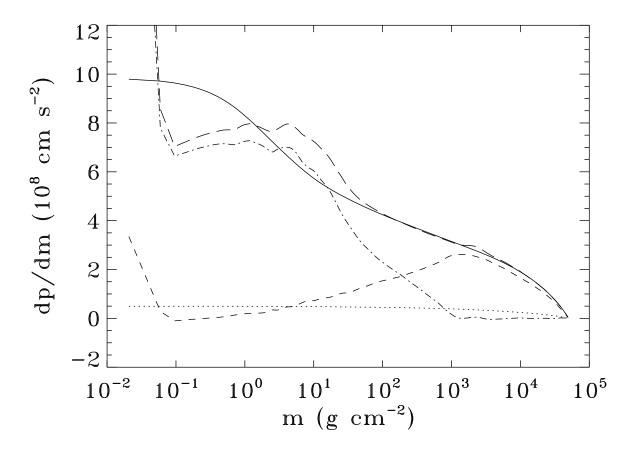


Fig. 3.— Time and horizontally-averaged profiles of vertical acceleration due to magnetic pressure gradients (dot-dashed), gas pressure gradients (short-dashed), and radiation pressure (dotted). The long-dashed curve shows the sum of these three accelerations, and should be compared to the magnitude of the gravitational acceleration (solid curve).

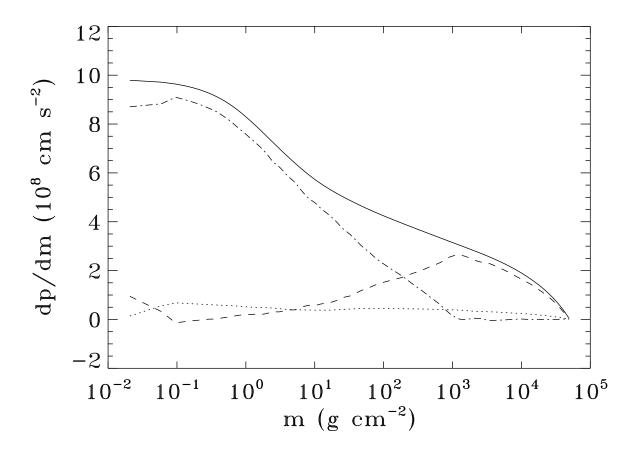


Fig. 4.— Rescaled, fractional contributions of the time and horizontally-averaged vertical acceleration due to magnetic pressure gradients (dot-dashed), gas pressure gradients (short-dashed), and radiation pressure (dotted). The local gravitational acceleration is shown by the solid curve.

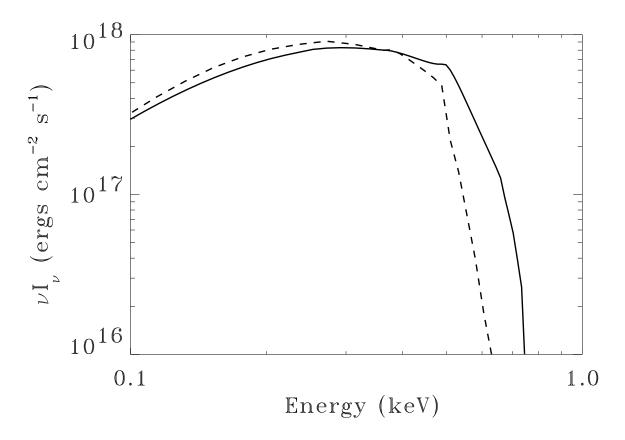


Fig. 5.— Local emergent spectrum in fluid rest frame from the disk annulus viewed at an inclination angle of  $55^{\circ}$  from the disk normal. The dashed curve neglects magnetic pressure support in the vertical hydrostatic balance, while the solid curve includes it. Both calculations assume the dissipation profile of equation (1).

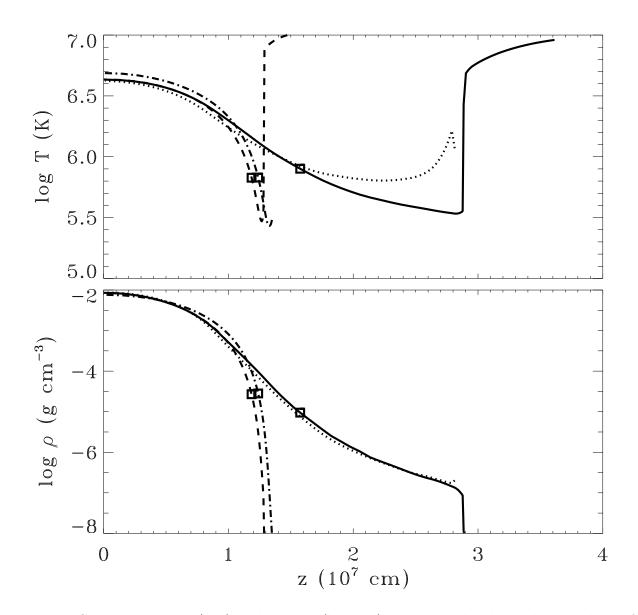


Fig. 6.— Gas temperature (top) and density (bottom) versus height above the midplane of the annulus. The solid curve includes the contribution of magnetic pressure support to the hydrostatic balance, while the dashed curve neglects it. Both curves assume the dissipation profile of equation (1). The dot-dashed curve is the structure that would be obtained under standard assumptions: no magnetic pressure support and a constant dissipation per unit mass. Squares mark the position of the effective photosphere for photon energies of 0.45 keV, which is near the peaks of the  $\nu I_{\nu}$  spectra shown in Figures 2 and 5. For comparison, the dotted curve shows the time and space-averaged temperature and density from the Hirose, Krolik, & Stone (2005) simulation.

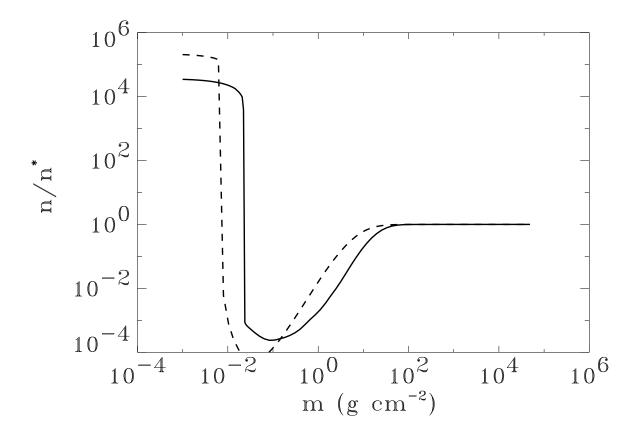


Fig. 7.— Ratio of the actual ground state number density n of CVI to the ground state number density  $n^*$  that would be present in LTE, as a function of column density. The solid curve includes the effects of magnetic pressure support, while the dashed curve neglects it. Both curves assume the numerical dissipation profile of equation (1). Magnetic pressure support results in greater departures from LTE at higher column densities.

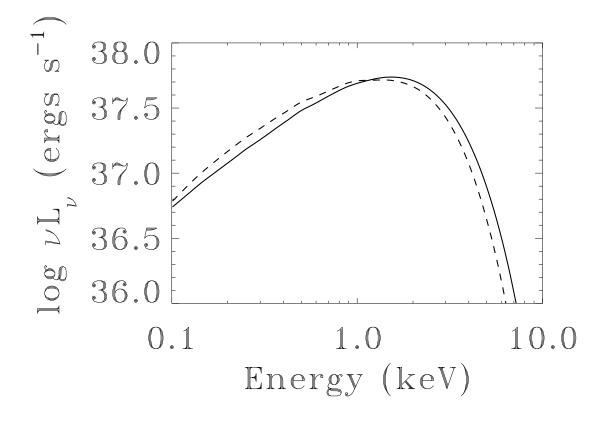


Fig. 8.— Spectrum of full relativistic accretion disk models with  $\alpha = 0.01$  and  $L/L_{\rm Edd} = 0.08$  orbiting a ten solar mass Schwarzschild hole, as viewed by an observer at infinity at 60° from the symmetry axis. Both models adopt the vertical dissipation profile given by equation (1). The solid curve includes magnetic pressure support, while the dashed curve neglects it.